Non-coding RNA Research 4 (2019) 121–127

Contents lists available at ScienceDirect

Non-coding RNA Research

journal homepage: http://www.keaipublishing.com/ncrna

Comprehensive structure-function analysis of causative variants in retinal pigment epithelium specific 65 kDa protein associated Leber Congenital Amaurosis

Zainularifeen Abduljaleel[a,b,c,*]

[a] Department of Medical Genetics, Umm Al-Qura University, P.O. Box 715, Makkah, 21955, Saudi Arabia
[b] Science and Technology Unit, Umm Al Qura University, P.O. Box 715, Makkah, 21955, Saudi Arabia
[c] Bircham International University, Av. Sierra, 2, 28691, Villanueva de La Cañada, Madrid, Spain

ARTICLE INFO

Keywords:
Leber congenital amaurosis (LCA)
RPE65
Structural and functional implication
Clinical implication
Mutation stability

ABSTRACT

A recent study published to screen *RPE65* in 187 families with Leber Congenital Amaurosis (LCA) by Zilin Zhong in 2019. There are seven novel variants were identified in *RPE65,* which was associated with LCA, but among only five were missense mutations [(c.124C > T, p.(Leu42Phe), c.149T > C, p. (Phe50Ser), c.340A > C, p. (Asn114His), c.425A > G, p.(Asp142Gly) and c.1399C > G, p.(Pro467Ala)] in the Chinese population and potentially facilitates its clinical implementation. Further in-continuation of this study to the target of five novel missense mutations were the analysis of both structural and functional impact by the molecular dynamics and simulation. The result of five missense mutations might in critical structural alterations of RPE65 protein, disrupt its membrane association or rescue the activity of enzyme due to thermodynamics stability, and for this reason impair its isomerohydrolase activity, resulting in retinal dystrophy. These observations suggest that the reduced protein stability and altered subcellular localization of RPE65 might signify a mechanism for these mutations to lead to vision loss in LCA patients.

1. Introduction

The retinal pigment epithelium (RPE) performs a number of functions critical for visual processing, metabolism, and survival of the photoreceptor cells of the retina [1]. Mutations in genes expressed in the RPE have recently emerged as an important cause of inherited retinal degeneration. *RPE65* was the first identified RPE-specific disease gene as a result of linkage studies that mapped the disease locus in a consanguineous family to the interval containing *RPE65* on chromosome 1p31 and identified mutations responsible for childhood-onset severe retinal dystrophy [2]. In addition, missense mutations in *RPE65* were identified in a patient with LCA type II by using the candidate gene approach [3]. Since these initial reports, a wide range of disease severity has been associated with *RPE65* mutations, from congenital blindness to adult-onset retinitis pigmentosa, although the most common phenotype is severe and early-onset retinal degeneration [4].

In humans, more than 100 mutations in *RPE65* have been identified associated with LCA, over all of the gene's 14 exons and their boundaries, up to half of which are missense mutations. Despite the broad spectrum of disease-causing mutations in *RPE65* in different populations, the spectrum of *RPE65* mutations reported is still narrow in the Chinese population [5] with a combination of different genotyping techniques and the published guidelines and standards of the American College of Medical Genetics (ACMG).

Aim of this study will investigation of five novel missense variants [(c.124C > T, p.(L42F), c.149T > C, p.(F50S), c.340A > C, p. (N114H), c.425A > G, p.(D142G) and c.1399C > G, p.(P467A)] to confirm by structural and functional analysis. Our findings include the thermodynamics protein stability and conformational changes by molecular dynamics simulations on a different millisecond timescale.

2. Materials and methods

2.1. Clinical dataset

The Institutional Review Board (IRB) of Tongji Eye Institute of Tongji University School of Medicine, (Shanghai, China) approved this study. In this study, a total of 187 unrelated retina specialists had diagnosed Chinese probands enrolled from the 16 provinces of China with LCA. Another cohort ascertained in this study as healthy control

* Department of Medical Genetics, Umm Al-Qura University, P.O. Box 715, Makkah, 21955, Saudi Arabia.
E-mail address: zaabduljaleel@uqu.edu.sa.

https://doi.org/10.1016/j.ncrna.2019.11.001
Received 29 October 2019; Received in revised form 7 November 2019; Accepted 8 November 2019
Available online 21 November 2019

comprised 200 ethnically matched unrelated individuals. Detailed ocular examinations and routine physical examinations were performed to obtain clinical data about these participants in this study. A variants data facilitate genetic counseling and the selection of patients with LCA who are eligible for therapeutic retinoid [5]. Furthermore, All variants were assessed by global variome shared LOVD database (https://databases.lovd.nl/shared/genes/RPE65).

2.2. Protein structure modeling

I-TASSER [6–8] modeling leads from the protein structure templates identified by LOMETS from the PDB library. LOMETS is a meta-server threading approach containing multiple threading programs, where each threading program can generate tens of thousands of template alignments. I-TASSER only uses the templates of the highest significance in the threading alignments, the significance of which are measured by Z-score, i.e. the difference between the raw and average scores in the unit of standard deviation. The templates in this section are the 10 best templates selected from the LOMETS threading programs. Usually, one protein model of the highest Z-score was selected from each threading, where the threading are sorted by the average performance in the large-scale benchmark test experiments.

2.3. Protein thermal stability changes

DynaMut [9] determined that implements two distinct well normal mode approaches, which can be used to analyse protein dynamics by sampling conformations as well as assess the impact of mutations on protein stability and dynamics. To study the dynamic nature and the role of flexibility and accessible conformational landscapes in proteins was essential for understanding their function, as well as to evaluate how changes in a protein might impact its structure, function and interactions, giving rise to different phenotypes. In addition, also assists rapid analysis of the effect of mutations on a protein's dynamics and stability resulting from vibrational entropy changes. Integration of these approaches well established methods and characteristics of the wild type residue environment into a consensus prediction to stipulate an accurate assessment of the impact of a mutation on protein stability, and require a comprehensive suite for protein motion and flexibility analysis. The results will be combines the effects of mutations on protein stability and dynamics calculated by program were ΔΔG mCSM [10], ΔΔG SDM [11], ENCoM [12] and ΔΔG DUET [13] to generate an optimized and more robust predictor.

2.4. Preparation of molecular dynamics (MD) simulation

The RPE65 structure model having 99% identity PDB ID: 3FSN was selected template for simulations computations the wild type structure of RPE65. Five mutants were generated starting from this wild type RPE65 protein structure: RPE65, where all residues (Leu42, Phe50, Asp142, N114, and P467) were mutated (42Phe, 50Ser, 142Gly, 114His, and 467Ala). These mutations were performed in Molecular Operation Environment (MOE). Similarly, Charmm [14] and Gromacs version 4.6.6 [15] performed all remaining steps for system preparations. Each structure was solvated in a water box having at least a 12 Å cushion of water in each direction from the exposed atoms. Ions were added to neutralize the system and set the NaCl concentration to 150 mM. Simulations were performed in Gromacs [16,17] using the force field.14 A cutoff distance of 12 Å was adopted for van der Waals (vdW) interactions, with a switching function starting at 10 Å and reaching 0 at 12 Å. Long-range electrostatic forces were computed using the particle-mesh Ewald method. A time step of 2 fs was used. Simulations were performed under isothermal-isobaric (NPT) ensemble conditions temperature and pressures were kept constant at 300 K and 1 atm, respectively. A damping coefficient of 1 ps−1 for Langevin dynamics was used to maintain isothermal conditions. The Langevin Nosé-Hoover method was performed using an oscillation period of 200 fs and a damping time scale of 100 fs to maintain the pressure constant. First, 10 000 steps of minimization followed by 2 ns of equilibration was performed by keeping the protein fixed. Subsequently, the complete system was finally minimized for additional 10 000 steps without any constrains/restrains on the RPE65 protein structure model. The resulting conformer was equilibrated for 6 ns where, during the first 2 ns of simulations, harmonic constraints having force constants of k = 2 kcal mol−1 Å−2 were applied to the backbone atoms. Each system was subsequently simulated for 720 ns and conformations were recorded every 100 ps hence, ending up with 14 400 conformers for each system.

3. Results

3.1. Clinical information

Leber congenital amaurosis is a group of hereditary in usually autosomal recessive retinal diseases also a rare hereditary retinal degeneration caused by mutations in more than a dozen genes are represent were Centrosomal protein of 290 kDa (CEP290) (15%), Guanylate cyclase 2D (GUCY2D) (12%), and Crumbs homolog 1 (CRB1) (10%) and Retinal pigment epithelium specific 65 kDa (RPE65) (8%) are the most frequently mutated was LCA genes. It was appears condition at birth or in the first few months of life with loss of vision, which varies from person to person and can be quite severe laterally no light perception. We studied representing of few cases data analysis from the existing clinical data server (Fig. 1), who has Leber congenital amaurosis associated with causative mutations with different condition.

3.2. Conserved domains and structural affect

Leber congenital amaurosis associated wild type residues c.124C > T, p.(L42F, and c.149T > C, p. (F50S) was very conserved, but a few other residues types have been observed at this position too. These residues were among the mutated residues at this position observed in other sequences. This means that homologous proteins exist with the same residue type as these two mutant and possibly not damaging to the protein by the structure. But it was near a highly conserved position. These two mutated residues were located in a domain of the same Carotenoid Oxygenase IPR0042924 that was more important for the activity of the protein and in contact with another domain that was also important for the activity. The interaction between these domains could be disturbed by the mutation, which might affect the function of the protein. This interaction may be important for the correct function of the protein. These mutations can affect the interaction and as such affect protein function as well. Therefore the local conformation will be slightly destabilized by the secondary mutated structure of the protein RPE65. The other three mutations c.340A > C, p.(N114H), c.425A > G, p.(D142G) and c.1399C > G, p.(P467A) of all wild type residues charge was negative, the charge of the mutant residues was neutral. All mutant residues are more hydrophobic than the wild type residues were highly conserved, but a few other residues have been observed at these positions. These mutated residues are located in the domain of Carotenoid Oxygenase IPR004294 that was also important for the activity of the protein and in contact with another domain. The interaction between these domains could be disturbed by these mutations, which might affect the function of the protein.

3.3. RPE65 mutations impact and thermal stability

Protein stability may directly relate to functional activity, and changes in stability or incorrect folding could be major consequences of pathogenic missense mutations. According to our recent findings RPE65 mutations in associated with Leber Congenital Amaurosis, that display high potential activity, may also induce the greater differential effect on

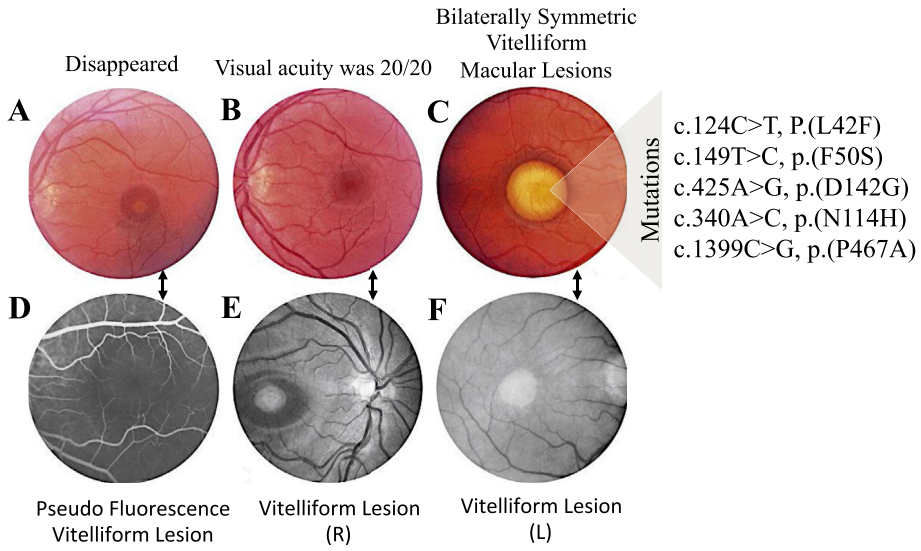

Fig. 1. A and B: A 19-year-old boy with the disease who complained of blurred vision in both eyes. His electro-oculographic findings were 1.00 in both eyes. Four months later the vitelliform lesions and surrounding retinal detachment (A) had disappeared (B). Visual acuity was 20/20. C and D: This 13-year-old female had bilaterally symmetric vitelliform macular lesions and visual acuity of 20/15. Angiograms showed minimal fluorescence of both eye lesions (probably pseudo fluorescence corresponding to the vitelliform lesion). E and F: A vitelliform lesion was present in both eyes of this 9-year-old boy (E) and in the right eye (F) of his 73-year-old grandfather who had a scar on the left macula.

Table 1
Predict stability effects of mutations on protein folding.

Protein model	Mutation	Type	Seq iden	Align score	Model	$\Delta G_{wt}^{(FoldX)}$	$\Delta G_{mut}^{(FoldX)}$	ΔΔG
RPE65	D142G	Core	0.998	0.998	−0.783	127.132	126.817	2.044
Human	F50S	Core	0.998	0.998	−0.783	127.602	127.625	2.296
	L42F	Core	0.998	0.998	−0.783	125.564	131.19	0.622
	N114H	Core	0.998	0.998	−0.783	127.716	127.748	−0.321
	P467A	Core	0.998	0.998	−0.783	127.65	130.229	1.217

thermodynamic stability of the wild and mutated forms of protein. These energetic factors may serve as thermodynamic stability stimulation by RPE65 mutations. In line with this hypothesis, structural signatures of the Leber Congenital Amaurosis mutational hotspot may manifest in deleterious protein stability changes in the inactive state of the interactive proteins, thereby promoting transitions to the constitutively active form. In the present study, we verified and expanded the initial inference by analyzing structural mapping of mutational hotspots and performing computational evaluation of protein stability changes by using one protein model with different mutations. The results of protein model are destabilizing folding, and expressed mutant *RPE65* protein shows altered mobility from the wilt type (Table 1). Currently, no clear consensus has emerged regarding *RPE65* palmitoylation, studies having suggested that *RPE65* does not undergo significant post-translational modifications. Finally, *RPE65* was the most biologically plausible candidate gene in the linkage region.

In addition, DynaMut method approaches revealed a consistent trend, whereby commonly occurring activating mutations with an appreciable response resulted in a considerable destabilization of the wild structure. For example, mutations p.(L42F), p. (F50S), p.(N114H), p. (D142G) and p.(P467A) from the mutational hotspot are known to have significant effect on the enzymatic activity or stability of this protein. Accordingly, these mutations were shown to have a significant destabilization effect on the protein structure. In order to illustrate functional significance of structural effects and concomitant protein stability changes for RPE65 mutations, we compared protein stability of those were two mutations P467A (0.12 kcal/mol) and N114H (1.159 kcal/mol) are Stabilizing by two different programs ΔΔG and ΔΔG SDM. Other than remaining all three mutations L42F, D142G, and F50S are destabilizing by another two ΔΔG mCSM and ΔΔG DUET (Table 2). The resulted of destabilizing mutations can clearly be deleterious as they are likely to cause structural modification which can negatively impact on protein function, it was less obvious that variants with a stabilizing effect can also be disease causing. These results are consistent supporting the hypothesis that functional role of IRE65 mutations may associated with their impact on the protein kinase stability.

3.4. Conformational changes in mutated protein and molecular dynamics simulation

This section will account for how mutation relates to the changes observed in translated regions of RPE65. At the point when the mutation shows a change in the translated protein (in exon) and regardless of whether it had an impact, there was missense mutation in the protein. Besides, it was identified that the test output was linked with RPE65 gene coding regions of the protein structure recovered from the Protein Data Bank (PDB), but point mutations are not covered within our region. So we settled the sequence from UniProtKB - Q16518 (RPE65_HUMAN). The structure prediction was determined by I-Tasser program. I-TASSER simulations generate a large ensemble of structural conformations by decoys. The final model protein was 99% structural similarity with PDB ID: 3FSN, selected based on the pairwise structure similarity, and the confidence of each model were quantitatively measured by C-score 1.60, TM-score 0.94 ± 0.05 and RMSD: 4.1 ± 2.7 Å that were calculated based on the significance of threading template alignments and the convergence parameters of the structure assembly simulations.

The RPE65 protein refined by 3Drefine to enhance topologies models as measured by based GDT-TS, TM-score and Cα RMSD to native structures and with a mutant. It's stated that the native state has typically been found at the lowest. The results of free energy and native-like conformations are represented at a lower energy in more analysis, the foremost native-like state was found usually to be at the lowest energy score comparing to different states, however not continuously as shown in Table 3.

However, the resulting structure arrangements for the merging parameters as to the structure grouping simulations. The RPE65 protein structure “Chain A” all mutations located on the alpha helix. On the

Table 2
The impact of mutations on protein stability and dynamics.

Gene	Mutation	PH	Temp	ΔΔG	Function	ΔΔG mCSM	Function	ΔΔG SDM	Function	ΔΔG DUET	Function
RPE65	P467A	7.0	25	0.17 kcal/mol	Stabilizing	−2.249 kcal/mol	Destabilizing	2.31 kcal/mol	Stabilizing	−1.303 kcal/mol	Destabilizing
Human	L42F	7.0	25	−0.12 kcal/mol	Destabilizing	−1.29 kcal/mol	Destabilizing	−0.66 kcal/mol	Destabilizing	−1.271 kcal/mol	Destabilizing
	D142G	7.0	25	−0.277 kcal/mol	Destabilizing	−0.453 kcal/mol	Destabilizing	1.46 kcal/mol	Stabilizing	0.196 kcal/mol	Stabilizing
	F50S	7.0	25	−2.189 kcal/mol	Destabilizing	−2.648 kcal/mol	Destabilizing	−3.28 kcal/mol	Destabilizing	−2.883 kcal/mol	Destabilizing
	N114H	7.0	25	1.159 kcal/mol	Stabilizing	−0.902 kcal/mol	Destabilizing	0.330 kcal/mol	Stabilizing	−0.812 kcal/mol	Destabilizing

Table 3
Protein structure refinements of different models with mutations.

#Models	Mutation	3Drefine Score	GDT-TS	GDT-HA	RMSD (Å)	MolProbity	RWPlus
RPE65	N114H	24366.8	0.9995	0.9883	0.288	2.663	−126278.1979
Human	D142G	24663.7	0.9995	0.992	0.268	2.624	−126180.1335
	F50S	25162	0.9995	0.9958	0.244	2.565	−125972.0931
	L42F	26182.5	1	0.9977	0.212	2.544	−125573.0482
	P46A	29602.2	1	0.9995	0.156	2.5	−125243.6242

Model # indicates the number of refinements on the model. 3Drefine Score: The potential energy of the refined model according to 3Drefine force filed.
GDT-TS and GDT-HA: Both similarity score in [0,1] of the refined model w.r.t the initial model and indicates conservative refinement.
RMSD: This is the CA-RMS deviation score in angstrom (Å) indicates aggressive refinement.
RWplus: This is the potential energy of the refined model according to RWplus statistical potential.
MolProbity: Physical realism score the refined model according to MolProbity score.

Table 4
Protein structure conformational changes by different time scale.

Mutation	RMS deviation	% Of native contacts	% Of non-native contacts	Contact order	# Of energy evaluations	# Of energy evaluations/sec	Time/sec
N114H	3.027	80.787	46.618	0.162	1503	15.76	95.55510187
D142G	4.025	77.48	51.383	0.151	5792	15.677	369.6336992
F50S	3.473	79.147	48.982	0.162	1730	16.069	107.796181
L42F	3.164	79.239	48.507	0.162	1664	16.762	99.44215298
P46A	4.288	78.549	50.595	0.154	4382	17.116	256.15992

other hand, mutations for relating positions were accomplished by using CCP4 (QtMG), which was identified fully to inspect the changed model structures. We check on the residues as well as on alpha-helix mutations analysis for RPE65. Later, the wild and mutant residues used for the MD simulation. The minimization energy of RPE65 receding mutations was performed at 300 800.706 kJ/mol and later lowered to −410 036.014 kJ/mol after completing the mutation as calculated by the help of MOE. Various polar and non-polar residues were used to screen and base the energy minimization procedures that enabled fixing a refinement cut of 0.00 Å with a reasonable solvent reduction. The consequence of diminishing the limited energy estimation of all wild type residues (Table 4) demonstrated that the mutant protein may add to enhance conservativeness and may inflate protein folding.

Additionally, mutations depended on the reasonable solvent as indicated by MD simulations. Amid these reenactments, proteins ceaselessly fold and unfold and give clear understanding for this procedure. When contrasted with the outcomes at a temperature of 300 K, the deviation of the RPE65 protein stretched from 2.0 Å to 10 ns. Interestingly, the deviation of all mutations was kept up at 1.2 Å until the simulation was completed (t = 10 ns). This determined that mutations had achieved its folded state while the little peak at 1.2 ns showed that mutations settled the protein structure. The resulting evidence demonstrated that the mutant structure was steady and could keep up its adaptation at 300 K, at a pressure bar of 1.00047. Besides, with a surface tension of 5000.0 Å, in an aggregate recreation time (ns) of 1.2/slipped by 0.0, and recording intervals (ps) energy of 1.2, in any case, there were inconspicuous changes that were seen between wild sort and mutant RPE65 protein. This can be seen when the superimposed structures with an RMSD estimation of 1.023 Å were resolved by use of MOE.

Other investigations of annotated anticipated solvent availability and pre-ascertained packing density revealed that mutant protein structure the density and reduce the intimate volume. The results of the mutations were contemplated utilizing a traditional molecular dynamics approach, whereby each of RPE65 wild and mutated structures was surveyed utilizing long simulation in an express solvent. The solvate distinguished the measurement of the framework with a set of water box changing to dissolve the molecule with an edge split-up of 10.0 Å. In the next level of normal mode dynamics to generate a consensus prediction of the impact of a mutation on protein stability and resulted from vibrational entropy changes of each structure in both complex of wild and mutant residues. A predict the effects of mutations on protein stability and flexibility (p-value < 0.001), achieving a correlation of up to 0.70, also for protein motion and flexibility with vibrational entropy energy values as shown in the Fig. 2.

4. Discussion

RPE65-associated retinal dystrophies comprise two different eye disorders, called retinitis pigmentosa and Leber congenital amaurosis. Both diseases are inherited in an autosomal recessive type and which can be caused by clinical significant variants in the gene RPE65. Although patients of different ethnicities have been reported, Leber congenital amaurosis was more severe than retinitis pigmentosa and manifests in infancy [18]. Patients have a profound loss of vision at an early age, and some have been reported to have an intellectual disability [19]. Life expectancy is not reduced, and no genotype to phenotype correlation has been noted as well. A corresponding of these five missense mutations p.(Leu42Phe), p.(Phe50Ser), p.(Asn114His), p.(Asp142Gly) and p.(Pro467Ala) as for reported based on Zilin Zhong et al., 2019, which was correlated with the Chinese cohort in a range of 1% (1/100) in LCA cases due to RPE65 mutations. This results overall

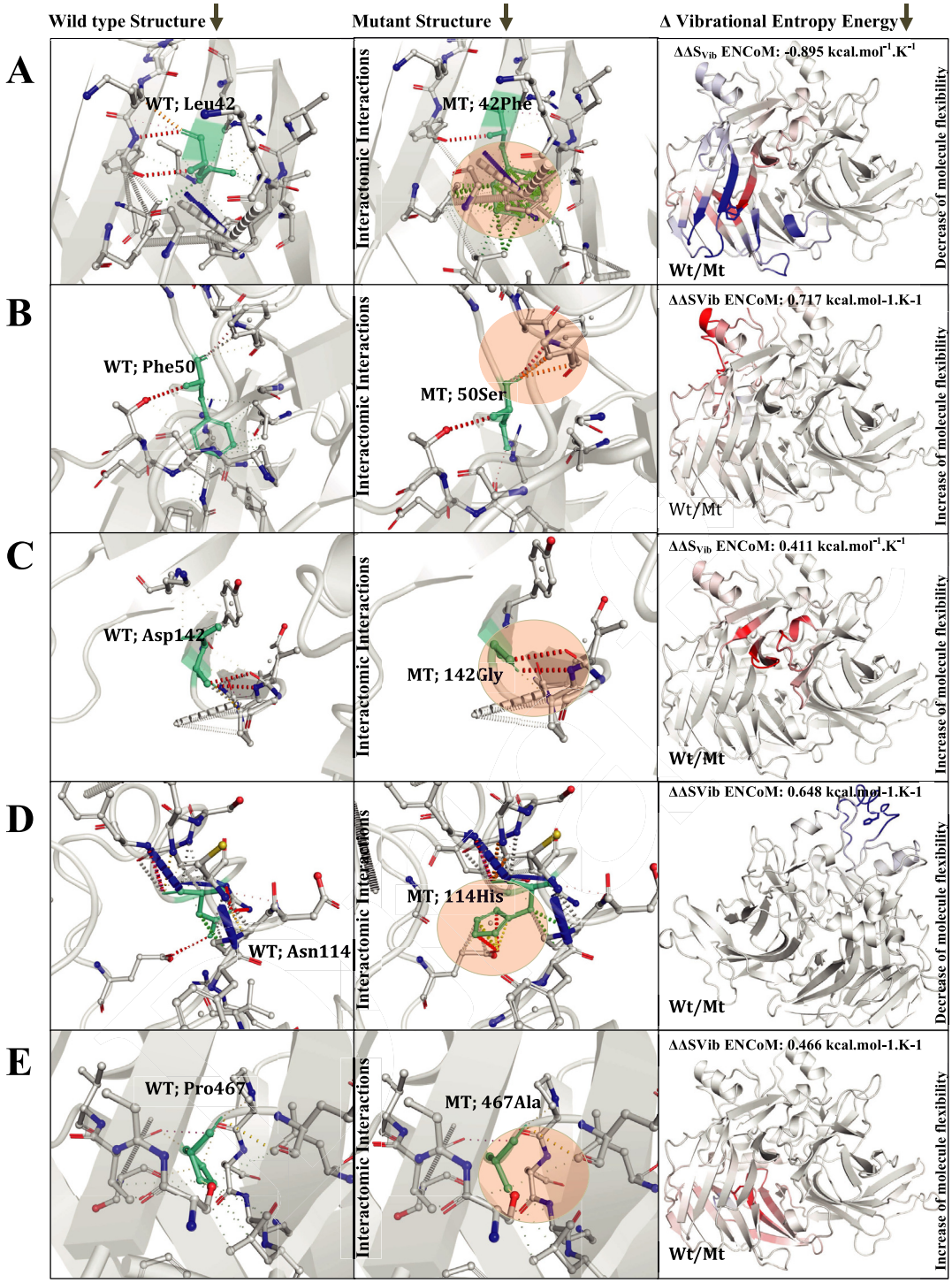

Fig. 2. A-E. Structure-based approaches for assessing the impact of mutations on protein structure and DynaMut determined function relying upon static. The protein dynamics by sampling conformations and assess the impact of mutations on protein dynamics and stability resulting from vibrational entropy changes of while in each wild and mutant residues conformational changes. All wild type and mutant residues are colored in light green and are also represented as sticks alongside with the surrounding residues, which are involved in any type of interactions also identity circle color in red. Other than each complex of wild and mutant of solvent accessibility by an accessible molecular surface, or solvent-exposed area, Amino acids colored according to the vibrational entropy change upon mutation. A blue represents a rigidification of the structure and red again in flexibility.

from India (1.7%) [20,21], Indonesia (9.5%) [22], Pakistan (4/146 = 2.7%) [23], and Kingdom of Saudi Arabia (4.4%) [21], but while compare with these four populations higher than from China (5.7%) [24]. A conceivable of the particular reason for these difference enrollment criteria. As for mutations in the RPE65 gene may be associated with LCA, in severe condition early childhood-onset retinal dystrophy of autosomal-dominant retinitis pigmentosa [25,26].

A critical stability framework can identify genetic mutations that will lead to LCA based on stability and function, and more specifically identify anything mutations are losses of function mutations [27].

Because changing critical residue leads to loss of protein stable structure, it was likely that these mutations lead to disease. There are five missense mutations that were qualitatively different from other pathogenic RPE65 mutations reported to date. LCA associated mutations are typically located not in the active site regions or at the interfaces of the beta sheet, but which may directly affect the protein function of the catalytic enzyme activity, folding trajectory or tertiary structure stability of the enzyme [28]. In mainly these three mutations P467A, D142G, and N114H provide evidence that all these three substitutions do not induce a protein-folding defect, similarly sparing any significant perturbation of the dynamic structure and catalytic activity of the protein. Instead, we find that it changes the thermodynamics stability of these all three mutant types residues were stabilizing and due to may produce an aggregation-prone surface capable of engaging giving chance in an abnormal protein-protein interactions. On the other hand we have a predisposition to shown with the L42F and F50S RPE65 mutants expressed in heterologous system that each were substitution caused destabilization of the protein, leading to accelerated degradation and complete lack of activity. This indisputable that L42 and F50 RPE65 has a important structural role within the RPE65 protein.

A MD simulations of protein folding {$\Delta G_{wt}^{(FoldX)}$ and $\Delta G_{mut}^{(FoldX)}$} [29] for this range of ~1–30 ms time scale are computationally heavy and currently were performed just one model with all mutated residues 42Phe, 50Ser, 114His, 142Gly and 467Ala. In our work, the proteins were equilibrated in water for ~100 ns. In this timespan only very earlier events of protein destabilization can be modeled. However, in the 100ns the protein were modeled were able to observe clear differences between structural conformational critical changes and delta critical changes to draw conclusions regarding the critical mutated residues' roles in creating the critical stability framework. These mutations molecule that can also may rescue the enzymes activity [30] By identifying the critical residues, we can better understand the chemistry of the protein and locate areas of the structure that may be modified to improve the binding chemistry of such small molecules. The idea of using mutagenesis to understand small molecule has already been explored [31]. As a computational technique, using critical residues can reduce the amount of time by identifying those residues that must remain in place for the protein to fold. Molecular dynamics was used to equilibrate the altered protein structure and show some possible stability changes may more stabilizing within the first 100 ns of simulation. These short simulations are not enough to see more significant differences, which we might expect at > 30 ms simulation for folding/unfolding processes. But a 'theoretically perfect' simulation technically was not possible because of technical limitations and accuracy of current computational methods. In a traditional multiple sequence alignments [32], the similarity of amino acid changes is not considered, rather only the identity of changes. This means that the conservation scores are calculated based on amino acid frequencies at a certain position in the alignment. This is a problem because some changes between similar residues maybe well tolerated.

Overall, this study limitation could be a problem as a result of some conformational changes between similar residues was also well tolerated. However, this may have to be analyzed in larger detail before conclusions will be reached. Finally, *RPE65* was most biologically plausible candidate gene in the linkage region. The RPE65 mutants are also accountable for the abolished activity of these five mutants. The mutants may have an effect on the RPE65 conformation that was essential for its enzymatic activity. Another chance of these five mutations might function key residues within the reactive site of the enzyme. Therefore, this study will not only make a case for however, RPE65 mutations impair vision in patients with retinal dystrophies, however provide signs for future RPE65 protein structure-function changes by molecular dynamics simulations on solvated biomolecular systems.

5. Conclusion

The altered of the mutant proteins RPE65, that contributed to there decreased stabilities and abolished enzymatic activities. However the structural changes of RPE65 resultant from these five mutations continue to be investigated, the current study demonstrates that destabilizing due to conformational changes of RPE65 started by mutations L42F and F50S could be accountable for the retinal degeneration in LCA patients. As there is no clinically satisfactory treatment for LCA and its pathogenesis is not completely understood, LCA remains a significant cause of inherited blindness. The present study has provided clues for further investigation of the pathogenesis of LCA and may contribute to the development of new therapies.

Declaration of competing interest

Authors declare there are no conflicts.

Acknowledgement

The author extends their appreciation to the Scientific Research at Umm Al-Qura University at Science and Technology Unit (STU). Makkah, Saudi Arabia.

References

[1] D. Bok, The retinal pigment epithelium: a versatile partner in vision, J. Cell Sci. Suppl. 17 (1993) 189–195.
[2] S.M. Gu, D.A. Thompson, C.R. Srikumari, B. Lorenz, U. Finckh, A. Nicoletti, et al., Mutations in RPE65 cause autosomal recessive childhood-onset severe retinal dystrophy, Nat. Genet. 17 (2) (1997) 194–197.
[3] F. Marlhens, C. Bareil, J.M. Griffoin, E. Zrenner, P. Amalric, C. Eliaou, et al., Mutations in RPE65 cause Leber's congenital amaurosis, Nat. Genet. 17 (2) (1997) 139–141.
[4] A.J. Lotery, P. Namperumalsamy, S.G. Jacobson, R.G. Weleber, G.A. Fishman, M.A. Musarella, et al., Mutation analysis of 3 genes in patients with Leber congenital amaurosis, Arch. Ophthalmol. 118 (4) (2000) 538–543.
[5] Z. Zhong, F. Rong, Y. Dai, A. Yibulayin, L. Zeng, J. Liao, et al., Seven novel variants expand the spectrum of, Mol. Vis. 25 (2019) 204–214.
[6] Y.I. ZhangT.A.S.S.E.R., Fully automated protein structure prediction in CASP8, Proteins 77 (Suppl 9) (2009) 100–113.
[7] A. Roy, J. Yang, Y. Zhang, COFACTOR: an accurate comparative algorithm for structure-based protein function annotation, Nucleic Acids Res. 40 (2012) W471–W477 Web Server issue.
[8] J. Yang, Y. Zhang, I-TASSER server: new development for protein structure and function predictions, Nucleic Acids Res. 43 (W1) (2015) W174–W181.
[9] C.H. Rodrigues, D.E. Pires, D.B. Ascher, DynaMut: predicting the impact of mutations on protein conformation, flexibility and stability, Nucleic Acids Res. 46 (W1) (2018) W350–W355.
[10] D.E. Pires, D.B. Ascher, T.L. Blundell, mCSM: predicting the effects of mutations in proteins using graph-based signatures, Bioinformatics 30 (3) (2014) 335–342.
[11] A.P. Pandurangan, B. Ochoa-Montaño, D.B. Ascher, T.L. Blundell, SDM: a server for predicting effects of mutations on protein stability, Nucleic Acids Res. 45 (W1) (2017) W229–W235.
[12] V. Frappier, M. Chartier, R.J. Najmanovich, ENCoM server: exploring protein conformational space and the effect of mutations on protein function and stability, Nucleic Acids Res. 43 (W1) (2015) W395–W400.
[13] D.E. Pires, D.B. Ascher, T.L. Blundell, DUET: a server for predicting effects of mutations on protein stability using an integrated computational approach, Nucleic Acids Res. 42 (2014) W314–W319 Web Server issue.
[14] S. Jo, X. Cheng, S.M. Islam, L. Huang, H. Rui, A. Zhu, et al., CHARMM-GUI PDB manipulator for advanced modeling and simulations of proteins containing non-standard residues, Adv. Protein Chem. Struct. Biol. 96 (2014) 235–265.
[15] B. Hess, C. Kutzner, D. van der Spoel, E. Lindahl, GROMACS 4: algorithms for highly efficient, load-balanced, and scalable molecular simulation, J. Chem. Theory Comput. 4 (3) (2008) 435–447.
[16] J. Comer, J.C. Phillips, K. Schulten, C. Chipot, Multiple-replica strategies for free-energy calculations in NAMD: multiple-Walker adaptive biasing force and Walker selection rules, J. Chem. Theory Comput. 10 (12) (2014) 5276–5285.
[17] B.R. Brooks, C.L. Brooks, A.D. Mackerell, L. Nilsson, R.J. Petrella, B. Roux, et al., CHARMM: the biomolecular simulation program, J. Comput. Chem. 30 (10) (2009) 1545–1614.
[18] R.J. Davis, C.W. Hsu, Y.T. Tsai, K.J. Wert, J. Sancho-Pelluz, C.S. Lin, et al., Therapeutic margins in a novel preclinical model of retinitis pigmentosa, J. Neurosci. 33 (33) (2013) 13475–13483.
[19] R. Bowman, The importance of assessing vision in disabled children - and how to do it, Community Eye Health 29 (93) (2016) 12–13.
[20] H. Morimura, G.A. Fishman, S.A. Grover, A.B. Fulton, E.L. Berson, T.P. Dryja,

Mutations in the RPE65 gene in patients with autosomal recessive retinitis pigmentosa or leber congenital amaurosis, Proc. Natl. Acad. Sci. U. S. A. 95 (6) (1998) 3088–3093.
[21] Y. Li, H. Wang, J. Peng, R.A. Gibbs, R.A. Lewis, J.R. Lupski, et al., Mutation survey of known LCA genes and loci in the Saudi Arabian population, Investig. Ophthalmol. Vis. Sci. 50 (3) (2009) 1336–1343.
[22] R.S. Sitorus, B. Lorenz, M.N. Preising, Analysis of three genes in Leber congenital amaurosis in Indonesian patients, Vis. Res. 43 (28) (2003) 3087–3093.
[23] M.I. Khan, M. Azam, M. Ajmal, R.W. Collin, A.I. den Hollander, F.P. Cremers, et al., The molecular basis of retinal dystrophies in Pakistan, Genes 5 (1) (2014) 176–195.
[24] L. Li, X. Xiao, S. Li, X. Jia, P. Wang, X. Guo, et al., Detection of variants in 15 genes in 87 unrelated Chinese patients with Leber congenital amaurosis, PLoS One 6 (5) (2011) e19458.
[25] R.G. Weleber, M. Michaelides, K.M. Trzupek, N.B. Stover, E.M. Stone, The phenotype of severe early childhood onset retinal dystrophy (SECORD) from mutation of RPE65 and differentiation from leber congenital amaurosis, Investig. Ophthalmol. Vis. Sci. 52 (1) (2011) 292–302.
[26] S.J. Bowne, M.M. Humphries, L.S. Sullivan, P.F. Kenna, L.C. Tam, A.S. Kiang, et al., A dominant mutation in RPE65 identified by whole-exome sequencing causes retinitis pigmentosa with choroidal involvement, Eur. J. Hum. Genet. 19 (10) (2011) 1074–1081.
[27] C.L. McCafferty, Y.V. Sergeev, In silico mapping of protein unfolding mutations for inherited disease, Sci. Rep. 6 (2016) 37298.
[28] G. Bereta, P.D. Kiser, M. Golczak, W. Sun, E. Heon, D.A. Saperstein, et al., Impact of retinal disease-associated RPE65 mutations on retinoid isomerization, Biochemistry 47 (37) (2008) 9856–9865.
[29] A. Sali, E. Shakhnovich, M. Karplus, How does a protein fold? Nature 369 (6477) (1994) 248–251.
[30] J.A. Zorn, J.A. Wells, Turning enzymes ON with small molecules, Nat. Chem. Biol. 6 (3) (2010) 179–188.
[31] K. Nishi, M. Ueno, Y. Murakami, N. Fukunaga, T. Akuta, D. Kadowaki, et al., A site-directed mutagenesis study of drug-binding selectivity in genetic variants of human alpha(1)-acid glycoprotein, J. Pharm. Sci. 98 (11) (2009) 4316–4326.
[32] M. Shatsky, R. Nussinov, H.J. Wolfson, Optimization of multiple-sequence alignment based on multiple-structure alignment, Proteins 62 (1) (2006) 209–217.